Novel Zinc Porphyrin Sensitizers for Dye-Sensitized Solar Cells: Synthesis and Spectral, Electrochemical, and Photovoltaic Properties

Cheng-Wei Lee,[a] Hsueh-Pei Lu,[b] Chi-Ming Lan,[b] Yi-Lin Huang,[a] You-Ren Liang,[a] Wei-Nan Yen,[a] Yen-Chun Liu,[a] You-Shiang Lin,[a] Eric Wei-Guang Diau,*[b] and Chen-Yu Yeh*[a]

Abstract: Novel *meso-* or β-derivatized porphyrins with a carboxyl group have been designed and synthesized for use as sensitizers in dye-sensitized solar cells (DSSCs). The position and nature of a bridge connecting the porphyrin ring and carboxylic acid group show significant influences on the spectral, electrochemical, and photovoltaic properties of these sensitizers. Absorption spectra of porphyrins with a phenylethynyl bridge show that both Soret and Q bands are red-shifted with respect to those of porphyrin **6**. This phenomenon is more pronounced for porphyrins **3** and **4**, which have a π-conjugated electron-donating group at the *meso* position opposite the anchoring group. Upon introduction of an ethynylene group at the *meso* position, the potential at the first oxidation alters only slightly whereas that for the first reduction is significantly shifted to the positive, thus indicating a decreased HOMO–LUMO gap. Quantum-chemical (DFT) results support the spectroelectrochemical data for a delocalization of charge between the porphyrin ring and the amino group in the first oxidative state of diarylamino-substituted porphyrin **5**, which exhibits the best photovoltaic performance among all the porphyrins under investigation. From a comparison of the cell performance based on the same TiO$_2$ films, the devices made of porphyrin **5** coadsorbed with chenodeoxycholic acid (CDCA) on TiO$_2$ in ratios [**5**]/[CDCA]=1:1 and 1:2 have efficiencies of power conversion similar to that of an **N3**-based DSSC, which makes this green dye a promising candidate for colorful DSSC applications.

Keywords: cross-coupling · donor–acceptor systems · electrochemistry · porphyrinoids · solar cells

Introduction

Dye-sensitized solar cells (DSSCs) have attracted much attention because they present a highly promising alternative to conventional photovoltaic devices based on silicon.[1] In nanocrystalline TiO$_2$ solar cells sensitized with a dye, efficiencies of conversion of light to electric power of up to 11% have been obtained with polypyridyl ruthenium complexes.[2] The advantages of using such ruthenium complexes are that they exhibit broad absorption in the near-UV and visible regions and appropriate excited-state oxidation potentials for electron injection into the conduction band of TiO$_2$.[3] The cost, rarity, and environmental issues of ruthenium complexes limit their wide application and encourage exploration of cheaper and safer sensitizers.

Considerable effort has been devoted to the development of new and efficient sensitizers suitable for practical use. Among these, organic sensitizers have drawn great interest because of their modest cost, ease of synthesis and modification, large molar absorption coefficients, and satisfactory stability. Organic dyes, such as coumarin,[4] indoline,[5] oligoene,[6] thiophene,[7] triarylamine,[8] perylene,[9] cyanine,[10] and hemicyanine[11] derivatives, have been investigated as sensitizers in DSSCs. Some organic dyes with conversion efficiencies in a range of 5–9% have been prepared.[5,12]

In the photosynthetic cores of bacteria and plants, solar energy is collected by chromophores based on porphyrin,[13]

[a] C.-W. Lee, Y.-L. Huang, Y.-R. Liang, W.-N. Yen, Y.-C. Liu, Y.-S. Lin, Prof. C.-Y. Yeh
Department of Chemistry
National Chung Hsing University
Taichung 402 (Taiwan)
Fax: (+886) 4-2286-2547
E-mail: cyyeh@dragon.nchu.edu.tw

[b] H.-P. Lu, C.-M. Lan, Prof. E. W.-G. Diau
Department of Applied Chemistry
National Chiao Tung University
Hsinchu 300 (Taiwan)
Fax: (+886) 3-572-3764
E-mail: diau@mail.nctu.edu.tw

Supporting information for this article, which contains the experimental details, is available on the WWW under http://dx.doi.org/10.1002/chem.200801572.

and the captured radiant energy is converted efficiently to chemical energy. Various artificial photosynthetic model systems have been designed and synthesized to elucidate the factors that control the photoinduced electron-transfer reaction.[14] Valuable knowledge has been acquired from these artificial systems. Inspired by the efficient energy transfer in naturally occurring photosynthetic reaction centers, numerous porphyrin[15] and phthalocyanine[16] dyes have been synthesized and used for photovoltaic solar cells. The best-performing porphyrin dyes have been reported to have conversion efficiencies in DSSCs in a range of 5–7%.[17] The efficiency of power conversion depends on how the sensitizer is attached to the surface of a semiconductor.[18]

To investigate how the structure of porphyrins affects the cell performance of devices, we have designed and synthesized novel carboxylated porphyrin-based sensitizers **1–5** and **7–12**, in which the porphyrin ring and the carboxyl anchoring group are connected with a vinyl, phenyl, or phenyl-ethynyl (PE) bridging unit at the *meso* or β position. Herein, we report the synthesis and the spectral, electrochemical, and photovoltaic properties of these porphyrin-based sensitizers. For comparison, porphyrin sensitizer **6** was prepared according to a literature method.[19] Our results in-

dicate that the cell performance of the device using porphyrin **5** as sensitizer outperforms the best-reported porphyrin dye and has a performance similar to that of an **N3**-based DSSC. Therefore, **5** might be a promising green dye for future colorful DSSC applications.

Results and Discussion

Design and synthesis: The major factor in decreasing the efficiency of sensitized photocurrent generation is the formation of dye aggregates on the semiconductor surface.[20] To decrease that aggregation, 3,5-di-*tert*-butylphenyl groups were introduced at the *meso* positions of the porphyrin ring. Our approach to the enhancement of absorption by porphyrin dyes in the visible region is to expand the π-conjugation system, which causes a red shift and broadening of both Soret and Q bands. In research on porphyrin arrays and porphyrin-based push–pull chromophores, bridges of the ethyne type have been shown to allow efficient conjugation and strong electronic interaction between chromophores, and to provide a well-defined and rigid structural arrangement.[21] We thus designed porphyrins with an ethyne bridging unit,
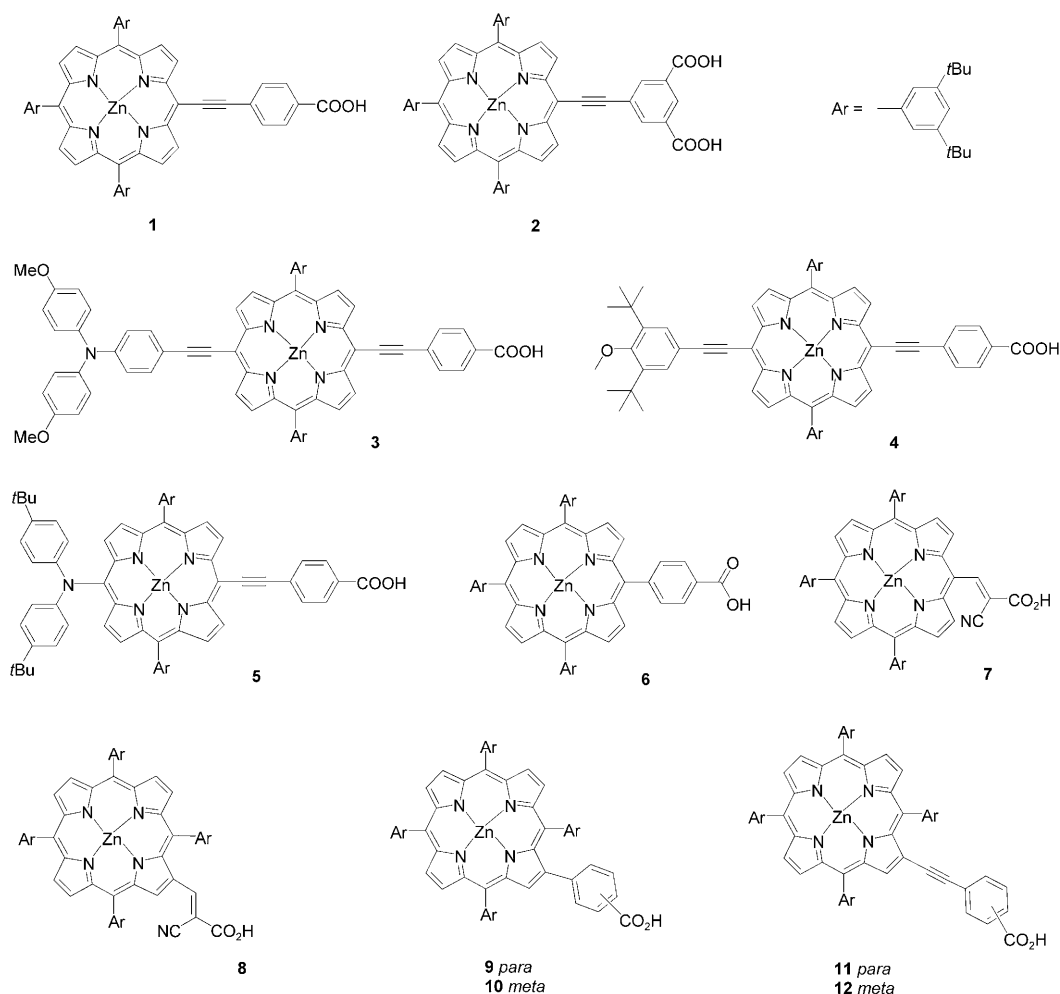
which might facilitate electron transfer from the excited dye to the TiO$_2$ surface, and which are expected to show an improved efficiency of energy conversion. The synthetic approach to these ethynyl-bridged porphyrins has been designed on the basis of Sonogashira coupling reactions. As an example, porphyrin **1** was obtained by Sonogoshira coupling of zinc 5-iodo-10,15,20-tris(3,5-di-*tert*-butylphenyl)porphyrin with 4-carboxyphenylethyne in satisfactory yield.[22]

Most highly efficient dyes used in DSSCs have a push–pull structure.[23] To increase the electron-donating ability of the porphyrin ring, compound **3** with a triarylamine moiety was designed. The synthesis of **3** involved stepwise Sonogashira coupling reactions. Porphyrin **5** with a diarylamine group at the *meso* position was synthesized according to the route in Scheme 1. Bromination[24] of porphyrin **13** with
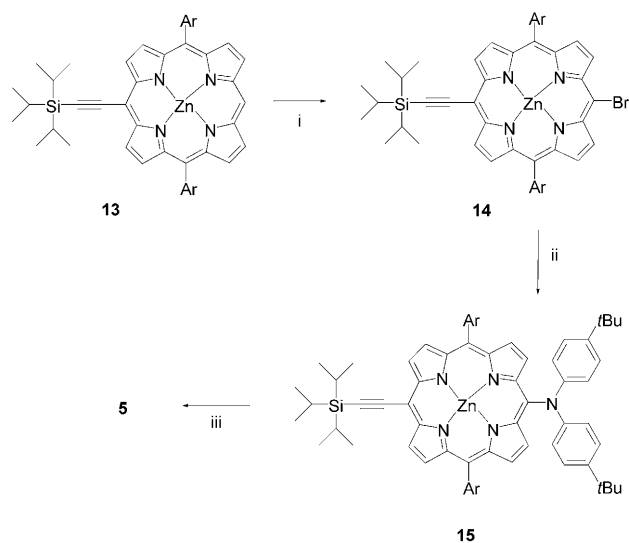
Scheme 1. Synthesis of **5**. i) NBS, CHCl$_3$. ii) Bis(4-*tert*-butylphenyl)amine, NaH, Pd(OAc)$_2$, DPEphos, THF. iii) TBAF, THF, RT; then 4-iodobenzoic acid, [Pd$_2$(dba)$_3$], AsPh$_3$, THF, NEt$_3$, reflux. NBS: *N*-bromosuccinimide, DPEphos: bis(2-diphenylphosphinophenyl)ether, TBAF: tetrabutylammonium fluoride, dba: dibenzylideneacetone.

NBS gave **14** in satisfactory yield; subsequent amination afforded **15**.[25] Deprotection of **15** with TBAF followed by Sonogashira coupling to 4-iodobenzoic acid produced porphyrin **5**.

An alternative approach to increase the domain of absorption in the visible region, and thus to increase the conversion efficiency, is to use a unit of ethenyl type as the linker.[26] The best porphyrin-based sensitizers, which exhibit efficiencies of energy conversion of 5%, are those with a β-substituted cyanoacetic or malonic acid, reported by Grätzel and co-workers.[17] We thus undertook the synthesis of porphyrins **7** and **8**, which have a cyanoacetic acid substituted at the *meso* and β positions, respectively, by employing a procedure similar to that reported by Grätzel et al.[17b]

The position and nature of the link between the porphyrin and the carboxyl group are expected to influence significantly the efficiency of energy conversion. Compounds **9–12**

with a phenyl or PE bridge at the β position were synthesized. Porphyrins **9** and **10** were obtained by Suzuki coupling of 2-bromo-5,10,15,20-tetrakis(3,5-di-*tert*-butylphenyl)porphyrin (**16**) to the corresponding phenylboronic acids.[27,28] Porphyrins **11** and **12** were prepared from reactions between **16** and the corresponding carboxylphenylethynes with Sonogashira coupling.

Spectral and electrochemical properties: The UV/Vis spectra of these compounds in solution exhibit the features typical of a porphyrin ring, with an intense Soret band in the range 400–500 nm and less intense Q bands in a range from 550 to 750 nm. As expected, the electronic absorption bands of porphyrins are sensitive to substituents on the periphery of the porphyrin ring. Examples of absorption spectra for porphyrins **1**, **3**, **5**, **6**, and **9** appear in Figure 1; UV/Vis data
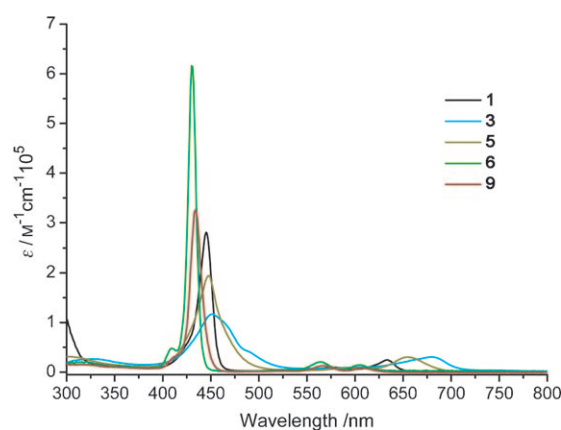
Figure 1. UV/Vis absorption spectra of **1**, **3**, **5**, **6**, and **9** in CH$_2$Cl$_2$/pyridine (100:1).

for each compound are summarized in Table 1. Comparison of the spectra of **9** and **10** with that of **6** reveals that substitution of carboxyphenyl at the β position causes no significant red shift of either Soret or Q bands because of an orthogonal orientation between the carboxyphenyl and porphyrin rings. For **11** and **12**, in which ethyne serves as the bridge between the porphyrin ring and anchoring group, the Soret and Q bands are more red-shifted than those of **9** and **10**. Perturbation of the energy of the HOMO and LUMO of the porphyrin ring is pronounced when *meso*- or β-ethenyl is employed as the linker, as indicated by significant broadening and a red shift of the absorption bands of porphyrins **7** and **8** relative to **9–12**. Compounds **1** and **2** show a similar spectral feature and substitution of carboxyphenyl at their *meso* positions by an ethyne linker that results in red shifts of the absorption bands which are larger than those for β-substituted analogues **11** and **12**. Compound **5** shows broadening of the Soret band and a red shift of the Q band relative to the spectrum of **1** due to electronic interaction between the diarylamino group and the porphyrin ring of **5**. Comparison of the absorption spectra of porphyrins **3** and **4** with that of **1** shows that red shifts and broadening increase

Table 1. Electronic absorption and emission data for porphyrins **1–12**.[a]

Porphyrin	Absorption λ_{max} [nm] (ε [10^3 M^{-1} cm^{-1}])	Emission λ_{max} [nm]
1	445 (282), 579 (9.5), 636 (24.8)	653[b]
2	445 (231), 582 (8.2), 632 (19.4)	651[b]
3	451 (117), 680 (30.6)	707[c]
4	454 (283), 668 (51.0)	687[c]
5	448 (194), 601 (8.3), 654 (29.7)	687[c]
6	430 (616), 565 (20.7), 605 (14.7)	617, 660[b]
7	455 (106), 571 (7.1), 636 (8.4)	659[d]
8	451 (129), 564 (11.7), 613 (11.1)	666[d]
9	434 (326), 567 (12.9), 607 (7.7)	631[b]
10	433 (409), 566 (16.3), 609 (10.7)	630[b]
11	442 (348), 574 (21.0), 618 (13.0)	635[b]
12	444 (375), 575 (25.1), 618 (16.3)	635[b]

[a] Absorption and emission data were measured for (CH$_2$Cl$_2$/pyridine = 100:1) solutions at 298 K. The excitation wavelengths were [b] 550 nm, [c] 650 nm, and [d] 600 nm.

systematically with increasing π conjugation.[29] A similar trend was observed in the fluorescence spectra.

We investigated the electrochemical properties of these porphyrins with cyclic voltammetry. Because the solubility of some of these porphyrins in CH$_2$Cl$_2$ was poor, we dissolved them in THF. In general, two oxidations and two reductions are expected for a zinc porphyrin under our electrochemical conditions. For some porphyrins, the oxidation waves were irreversible under ambient conditions; the electrochemical reactions of these porphyrins were therefore investigated at low temperatures. The measured oxidation and reduction potentials of these porphyrins are listed in Table 2. Figure 2 shows examples of cyclic voltammograms

Table 2. Electrochemical data for porphyrins **1–12**.[a]

Porphyrin	Oxidation $E_{1/2}$ [V]	Reduction $E_{1/2}$ [V]
1	+1.00	−1.19
2	+1.05[b]	−1.24
3	+0.86, +1.02	−1.08
4	+0.98	−1.06
5	+0.87[a] (+0.79, +1.05, +1.73)[c]	−1.11[a] (−1.02)[c]
6	+0.96	−1.36
7	+1.03	−1.21[b]
8	+0.98	−1.36[b]
9	+1.04[b]	−1.41
10	+0.95	−1.35
11	+1.00	−1.36[b]
12	+0.99	−1.40[b]

[a] Electrochemical measurements were performed at −20°C in THF containing TBAPF$_6$ (0.1 M) as supporting electrolyte. Potentials [V] are reported versus Ag/AgCl and reference to the ferrocene/ferrocenium (Fc/Fc$^+$) couple (THF, −20°C, +0.57 V). [b] Irreversible process E_{pa} or E_{pc}. [c] Electrochemical measurements were performed at −20°C in CH$_2$Cl$_2$ containing TBAPF$_6$ (0.1 M) as supporting electrolyte.

for porphyrins **1**, **4**, and **6** in THF containing tetrabutylammonium hexafluorophosphate (TBAPF$_6$; 0.1 M) at −20°C. For porphyrin **1**, the first oxidation at $E_{1/2}$(ox1) = +1.00 V and the first reduction at $E_{1/2}$(red1) = −1.19 V are reversible.

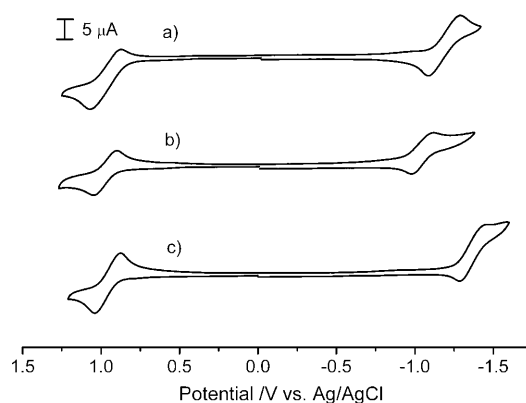Figure 2. Cyclic voltammograms of a) **1**, b) **4**, and c) **6** in THF containing 0.1 M TBAPF$_6$.

The electron-withdrawing property of the carboxyl anchoring group through a PE linker in **1** has no significant influence on its oxidation potential. The first oxidation is shifted only slightly by 40 mV to the positive relative to porphyrin **6**; we attribute this property to the strong electronic interaction between the carboxyl group and the porphyrin macrocycle through the PE linker, which allows positive charge to delocalize over the PE unit upon oxidation. The effect of the electron-withdrawing ability of the carboxyl PE linker on the oxidation potential is thus partially compensated by the charge delocalization. In contrast, the significant shift of the first reduction of **1** versus **6** by 170 mV to the positive indicates that both electron withdrawal and electronic delocalization influence the reduction potential in the same direction. A similar trend of the reduction potentials of **4** was also observed. As shown in Table 2, the half-wave potentials for the first abstraction of an electron from the porphyrin ring, except for **3** and **5**, are in a small range +0.96 to +1.05 V, whereas those for the first reduction span a large range of −1.06 to −1.41 V. The electrochemical HOMO–LUMO energy gap decreases as the π conjugation is extended, consistent with red shifts of both Soret and Q bands in the electronic absorption spectra. The potential for the first oxidation of porphyrins corresponds to the HOMO level. The LUMO energy level is predictable from the HOMO and the absorption threshold. In our new porphyrins, the LUMO levels are more negative than the conduction-band edge (−0.5 V vs. normal hydrogen electrode) and the HOMO levels are more positive than the oxidation potential for I$^-$/I$_3^-$, which meets the requirement for effective electron injection and dye regeneration in a DSSC system.[1–3]

The cyclic voltammogram of **3** shows that the first and second 1-e$^-$ oxidations, $E_{1/2}$(ox1) = +0.86 and $E_{1/2}$(ox2) = +1.02 V, overlap, which one can resolve by using differential pulse voltammetry (Figure 3). The first reduction of the porphyrin ring was observed at −1.08 V. The oxidation centers are identified by comparison with those of the corresponding triarylamine and porphyrin components, with reduction at $E_{1/2}$ = +0.91 and +0.99 V, respectively. The first oxidation
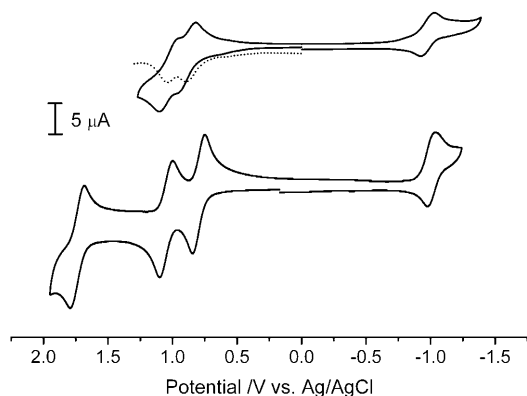
Figure 3. Cyclic voltammogram (——) and differential pulse voltammogram (-----) of **3** (top) in THF and cyclic voltammogram of **5** (bottom) in CH$_2$Cl$_2$ containing TBAPF$_6$ (0.1 M) at −20 °C.

of **3** at $E_{1/2}$(ox1) = +0.86 thus corresponds to one electron being abstracted from the triarylamine unit; the second abstraction at $E_{1/2}$(ox2) = +1.02 V corresponds to oxidation of the porphyrin ring. The assignments of these oxidation centers for compound **3** are confirmed with thin-layer spectroelectrochemistry, as discussed below.

Compound **5** shows two reversible reactions at potentials +0.87 and −1.11 V in THF at −20 °C for the first oxidation and first reduction, respectively, but in CH$_2$Cl$_2$ porphyrin **5** exhibits three reversible couples at potentials $E_{1/2}$ = +0.79, +1.05, and +1.73 V, which correspond to oxidations from the amino functional group and the porphyrin ring; the first reduction of the porphyrin ring was observed at a potential of −1.02 V. To identify the redox centers, we performed quantum-chemical calculations on **5** by density functional theory (DFT) at the B3LYP/6-31G(d) level (Spartan '06 package). As shown in Figure 4, the electron density of **5** is
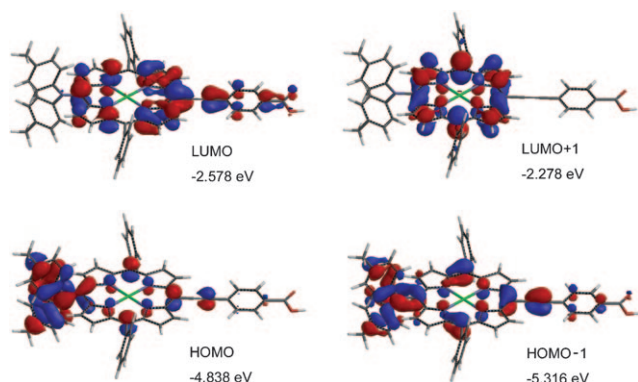

Figure 4. Surfaces of frontier molecular orbitals of **5** predicted with DFT calculations. To simplify the computations, *tert*-butyl groups at the *para* and *meta* positions were replaced with methyl groups and hydrogen atoms, respectively.

significantly distributed to the π system of the porphyrin ring, the diphenylamino moiety, and the PE linker at the HOMO and HOMO-1, but the π conjugation is extended to

only the porphyrin ring and the PE linker at the LUMO; LUMO+1 shows the localization of electron density solely on the porphyrin ring. Both diarylamino and porphyrin units are hence responsible for the first and second oxidations at $E_{1/2}$ = +0.79 and +1.05 V. In contrast, the reduction at $E_{1/2}$ = −1.02 V involves charge delocalization only on the porphyrin ring and the PE linker, thus facilitating electron transfer from the dye to TiO$_2$ through the linker.

Regarding electron transfer in DSSCs, absorption of a photon promotes an electron from the ground state of the dye into an excited state. The electron is then transferred from the excited dye to the semiconductor on an ultrarapid timescale. The interfacial electron transfer between the excited dye and the TiO$_2$ semiconductor can be investigated by detection of the temporally resolved absorption signals of dye cations through spectrometric techniques. To gain insight into the electronic absorption properties of the oxidized species of the sensitizers, we studied electrochemical reactions of compounds **1**, **3**, and **5** with a spectroelectrochemical method.[30] Thin-layer UV/Vis absorption spectra of porphyrin **1** recorded during electrochemical oxidation at an applied potential of +1.26 V in THF containing TBAPF$_6$ (0.1 M) at −20 °C are displayed in Figure 5. Scans of UV/Vis

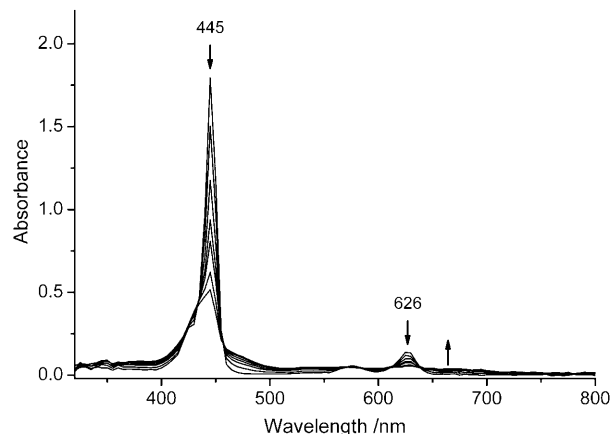Figure 5. Spectral changes of **1** in THF containing TBAPF$_6$ (0.1 M) at an applied potential of +1.26 V at −20 °C.

spectra at +1.26 V show that the intensities of the Soret and Q bands decrease significantly; furthermore, the Soret band broadens and a new and broad band appears at about 660 nm, which is characteristic of the formation of the porphyrin cation radical. The electrochemical oxidation is reversible because the porphyrin cation generated at +1.26 V can be reconverted to its neutral form in a ratio >90 % at an applied potential +0.80 V.

The oxidative electrolysis of porphyrin **3** was also performed at low temperature because the oxidized species was unstable under electrolysis at ambient temperature. Figure 6 shows the spectral changes of porphyrin **3** at applied potentials of +0.95 and +1.24 V in THF containing TBAPF$_6$ (0.1 M) at −20 °C. In the first oxidation, the signal at 332 nm
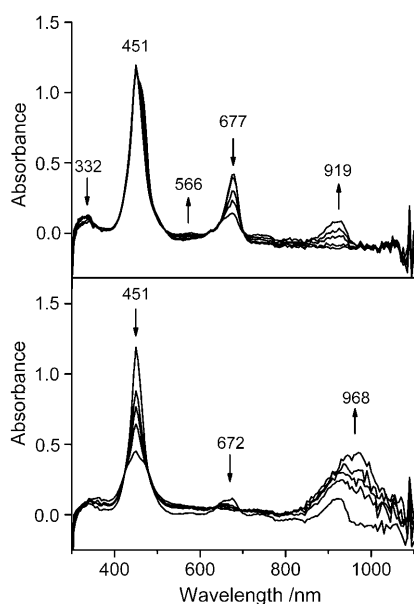
Figure 6. Spectral changes of **3** in THF containing TBAPF$_6$ (0.1 M) at applied potentials of +0.95 V (top) and +1.24 V (bottom) at −20 °C.

corresponding to the triarylamine unit decreases while that at about 566 nm, attributed to formation of the triarylamine cation, increases. The intensity of the Q band at 677 nm decreases and a new band at about 920 nm arises with clear isosbestic points. One-electron oxidation of a porphyrin ring generally results in a significantly decreased intensity of the Soret band, but in this case we observed sharpening and a slightly increased intensity of the Soret band upon 1−e^- oxidation. The first oxidation is hence assigned to a triarylamine-centered electrochemical reaction. Our previous work showed that the introduction of a triarylamine unit onto a porphyrin ring through an ethyne linker results in broadening and a red shift of the absorption bands because of strong electronic communication between the porphyrin and triarylamine units.[30] Upon oxidation of the triarylamine moiety, the sharpening and increased intensity of the Soret band might be ascribed to the decreased interchromophoric interaction between the porphyrin ring and the triarylamine cation. Further oxidation of porphyrin **3** at an applied potential of +1.24 V leads to a significantly decreased Soret band and extinction of the Q band, which are characteristics of a porphyrin-centered oxidation, and the presence of an intense near-IR band in the range 800–1100 nm. We reported previously the electrochemical and spectroelectrochemical properties of porphyrin–triarylamine conjugates, and a similar near-IR band has been observed upon oxidation of the conjugates.[29] These electrochemical oxidations are essentially reversible as more than 90 % of the oxidized species generated at +1.24 V can be reconverted to the neutral form of porphyrin **3** according to the intensity of the Q band.

We performed spectroelectrochemical measurements on compound **5** in CH$_2$Cl$_2$ because the 2−e^- oxidized species (**5**$^{2+}$) were unstable in THF even at −20 °C. In the first 1−e^-

oxidation ($E_{appl.}$ = +0.94 V), the absorption bands at 441 and 647 nm corresponding to the porphyrin ring and the band at 303 nm corresponding to the amino unit decrease, whereas those at 807 and 1384 nm increase with several clear isosbestic points (Figure 7). As mentioned for compound **3**, the
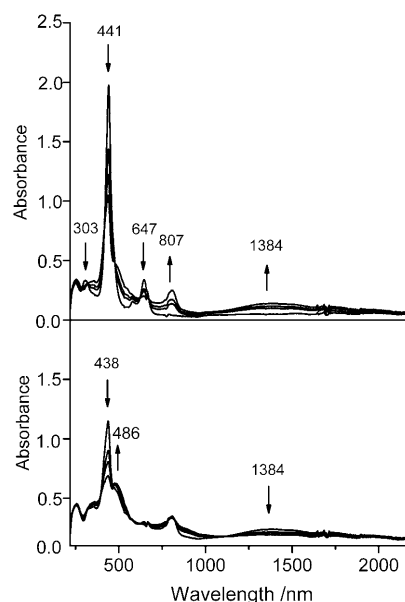

Figure 7. Spectral changes of **5** in CH$_2$Cl$_2$ containing TBAPF$_6$ (0.1 M) at applied potentials of +0.94 V (top) and +1.20 V (bottom) at −20 °C.

first electron abstraction occurs essentially from the triarylamine unit for which a significantly decreased Soret band was not observed. In contrast, both the Soret band and the band at 303 nm of compound **5** show a significant decrease upon abstraction of the first electron, indicating that the positive charge was delocalized over both the porphyrin ring and the amino unit. Further oxidation at an applied potential $E_{appl.}$ = +1.20 V resulted in decreased signals at 438 and 1384 nm and an increased band at 486 nm. These spectroelectrochemical results are consistent with those obtained from the quantum-chemical calculations; that is, the electronic densities of HOMO and HOMO−1 are distributed to both the porphyrin and diarylamine units discussed earlier.

Cell fabrication and photovoltaic characteristics: The porphyrins were sensitized onto TiO$_2$ nanoparticulate films to serve as working electrodes in DSSC devices. The TiO$_2$ nanoparticles (size ≈20 nm), prepared with a sol–gel method,[2b,31] were screen-printed onto the F-doped SnO$_2$ (FTO, 30 Ω cm^{-2}, Sinonar, Taiwan) glass substrate.[32] Crystallization of TiO$_2$ films (thickness ≈9 μm and active area 0.16 cm^2) was performed by annealing in two stages: heating at 450 °C for 5 min followed by heating at 500 °C for 30 min. The TiO$_2$ film was then immersed in an aqueous solution of TiCl$_4$ (50 mM, 70 °C, 30 min) followed by the same two-stage thermal treatment for final annealing of the electrode. The electrode was then immersed in a porphyrin/ethanol solu-

tion (0.2 mM, 25 °C, 2 h) containing chenodeoxycholic acid (CDCA; 0.2 mM unless otherwise specified) for dye loading onto the TiO$_2$ film. The Pt counter electrodes were prepared by spin-coating drops of H$_2$PtCl$_6$ solution onto FTO glass and heating at 400 °C for 15 min. To prevent a short circuit, the two electrodes were assembled into a cell of sandwich type and sealed with a hot-melt film (SX1170, Solaronix, thickness 25 μm). The electrolyte solution containing LiI (0.1 M), I$_2$ (0.05 M), 1-butyl-3-methylimidazolium iodide (0.6 M), and 4-*tert*-butylpyridine (0.5 M) in a mixture of acetonitrile and valeronitrile (volume ratio 1:1)[17b] was introduced into the space between the two electrodes, so completing the fabrication of these DSSC devices.

Through measurement of an *I–V* curve with an air mass (AM) 1.5 solar simulator (Newport–Oriel 91160), we assessed the performance of a DSSC device. The solar simulator uses filters and other optical components to mimic solar radiation with an AM 1.5 spectrum; the output intensity is evenly distributed for illumination of a large area. When the device is irradiated with the solar simulator, the source meter (Keithley 2400, computer-controlled) sends a voltage (*V*) to the device, and the photocurrent (*I*) is read at each step controlled by a computer through a general-purpose interface bus. The solar simulator was calibrated with a Si-based reference cell (S1133, Hamamatsu) and an IR filter (KG5) to correct the spectral mismatch of the lamp.[33] The efficiency (*η*) of conversion of light to electricity is obtained with the relations [Eq. (1)]:

$$\eta = \frac{P_{mp}}{P_{in}} = \frac{J_{mp}V_{mp}}{P_{in}} = \frac{J_{SC}V_{OC}FF}{P_{in}} \tag{1}$$

in which P_{in} is the input radiation power (for one solar radiation $P_{in}=100$ mW cm^{-2}) and P_{mp} is the maximum output power ($=J_{mp} \times V_{mp}$); the fill factor (*FF*) is defined as [Eq. (2)]:

$$FF = \frac{J_{mp}V_{mp}}{J_{SC}V_{OC}} \tag{2}$$

J_{SC} (mA cm^{-2}) is the current density measured at short circuit, and V_{OC} (V) is the voltage measured at open circuit. We classified compounds **1–11** into three categories (Figure 8); compound **12** was not measured because poor cell performance is anticipated for the anchoring groups in
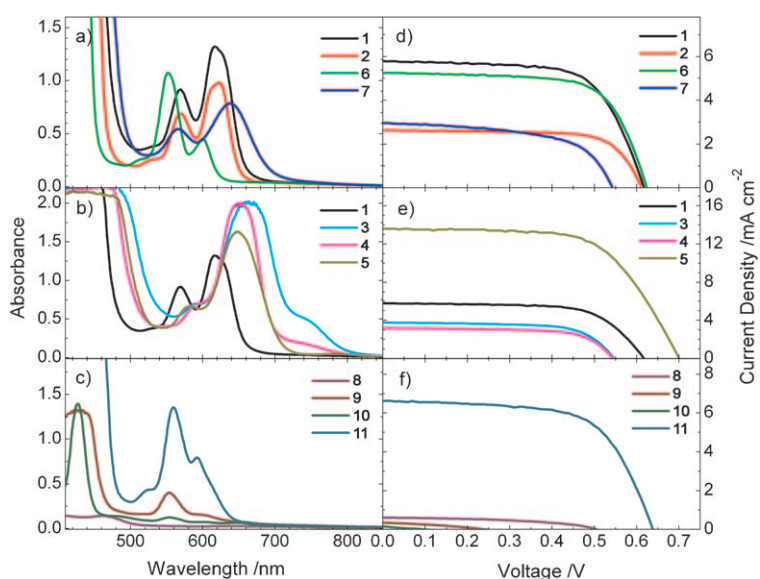

Figure 8. a)–c) Visible absorption spectra of porphyrin-sensitized TiO$_2$ with sensitizers **1–11**; d)–f) *I–V* curves of porphyrin-sensitized solar cells made of the corresponding sensitizers as in (a)–(c) under AM 1.5 illumination (power 100 mW cm^{-1}).

the *meta* positions. The absorption spectra of the porphyrin/TiO$_2$ films and the corresponding *I–V* curves of the solar cells made of the same sensitized films are shown in Figure 8a–c and 8d–f, respectively; the corresponding photovoltaic parameters are summarized in Table 3.

Table 3. Photovoltaic parameters of porphyrin-based DSSCs under AM 1.5 illumination (power 100 mW cm^{-2}) and active area 0.16 cm^2.[a]

Dye	J_{SC} [mA cm^{-2}]	V_{OC} [mV]	*FF*	*η* [%]
1	5.79	617	0.667	2.4
2	2.63	613	0.719	1.2
3	3.76	546	0.672	1.4
4	3.17	544	0.680	1.2
5	13.60	701	0.629	6.0
6	5.24	624	0.685	2.2
7	2.94	543	0.582	0.93
8	0.60	505	0.468	0.14
9	0.34	242	0.335	0.03
10	0.17	141	0.250	<0.01
11	6.61	638	0.642	2.7

[a] The photovoltaic parameters were obtained by fitting the corresponding current–voltage curves of Figure 8d–f according to Equation (1). For each sensitizer, two to four different devices of equal quality were tested and the uncertainties of *η* were within 10 %.

With compound **1** as our standard, we compared the cell performance for each porphyrin sensitizer. Compound **8** was designed to mimic the molecular structure of **Zn-3**,[17b] in which the COOH group is attached to the β position through a vinylene group, but incorporating the *tert*-butyl substituents to avoid dye aggregation. As shown in Figure 8c, compound **8** with a short linker attached at the β position of the porphyrin ring exhibits poor adsorption on the TiO$_2$ film, which causes poor cell performance (Figure 8f); compounds **9** and **10** similarly showed small efficiencies of

power conversion for the same reason—that the steric hindrance of the bulky *tert*-butyl groups impedes adsorption of the dye on TiO_2.

For compound **11** with a longer linker at the β position that promoted sufficient dye to become adsorbed on the TiO_2 film (Figure 8c), the efficiency of power conversion became comparable to that of compound **1** ($\eta = 2.7$ vs. 2.4%), thus indicating that the cell performance of a porphyrin-sensitized solar cell was insensitive to the position of the PE linker attached at the β or *meso* position. This result, although contrary to reported data,[17a] provides new evidence that *meso*-substituted porphyrins might serve as potential photosensitizers in DSSC applications. In what follows, we discuss the photovoltaic performance of devices fabricated with various *meso*-substituted porphyrins.

First, comparison of **1** and **2** shows that the anchoring group (COOH) in the *para* position performs better than that in the *meta* position ($\eta = 2.4$ vs. 1.2%), consistent with literature results.[17a] Relative to compound **1**, the structure of **6** lacks a triple bond in the linker so that its π conjugation is decreased. The Q band of **6** thus became blue-shifted and the photocurrent density of **6** decreased slightly relative to **1**. As a result, the power-conversion efficiency of **6** became slightly less than that of **1** (2.2 vs. 2.4%). In contrast, the Q band of **7** is red-shifted relative to **1** because the structure of **7** has an additional cyano group. The poor performance of **7** in both J_{SC} and V_{OC} leads to the power-conversion efficiency being much less than that of **1**. We expect that the superior electron-pulling capability of the cyano group in **7** might first pull the electrons and then transfer them back into the porphyrin core through space; this process is impracticable for **8** or **Zn-3**, in which the linker is attached to the β position.

To improve the charge separation in the sensitizer, we modified the structure of compound **1** by adding an efficient electron-pushing group at the *meso* position of the porphyrin ring, and designed porphyrins **3**–**5** accordingly. The additional triple bond in **3** and **4** extends the absorption to the near-IR region (Figure 8b), which might facilitate harvesting of sunlight toward a more efficient region, but **3** and **4** are poorly soluble in ethanol, thus leading to molecular aggregation in solution. The Q band of compound **3** adsorbed on TiO_2 became broad, an indication of serious dye aggregation on the surface of the TiO_2 films. As a result, the cell performances of both **3** and **4** were poorer than that of **1**. In contrast, porphyrin **5** with a diarylamino group attached directly at the *meso* position exhibited an excellent cell performance with $J_{SC} = 13.60$ mA cm^{-2}, $V_{OC} = 0.701$ V, $FF = 0.629$, and overall $\eta = 6.0\%$ obtained for a TiO_2 film of thickness ≈ 9 μm. The photocurrent density of **5** is more than twice that of **1**, indicating the superior capabilities of light harvesting and charge separation of that dye. The open-circuit voltage of **5** is notably the largest among all porphyrins under investigation.

We used CDCA as a coadsorbate for dye loading to prevent aggregation of the dye on the TiO_2 surface.[17b] The ratios of the concentrations of compound **5** and CDCA were
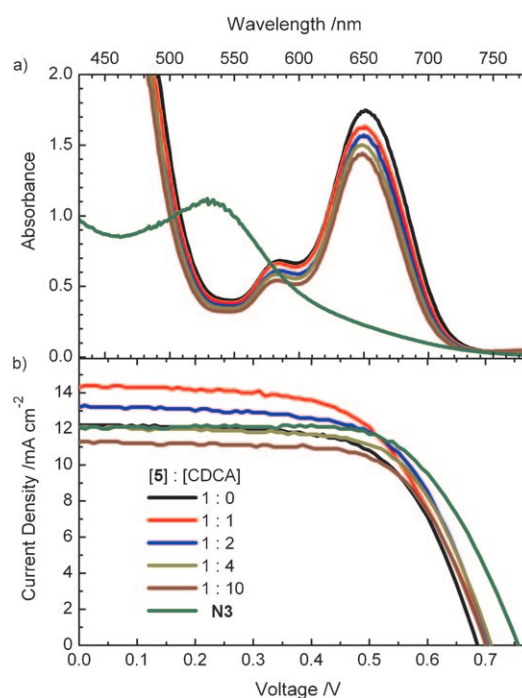

Figure 9. Comparison of the a) visible absorption spectra and b) *I–V* characteristics of porphyrin **5**-sensitized solar cells under different concentrations of coadsorber, CDCA.[17b]

varied as 1:0, 1:1, 1:2, 1:4, and 1:10; the corresponding dye/TiO_2 absorption spectra are shown in Figure 9a. Figure 9b compares the *I–V* characteristics of the devices made of porphyrin **5** under various dye/CDCA ratios, and the corresponding photovoltaic parameters are summarized in Table 4.

Our results indicate that treating with the coadsorbate CDCA together with loading the dye on TiO_2 films helps to impede dye aggregation, which increases both J_{SC} and V_{OC} and thus also η values; the best cell performance of a CDCA-treated device is for a cell with a dye/CDCA ratio between 1:1 and 1:2. Specifically, we found that the CDCA coadsorbates occupied effectively the available space on the TiO_2 surface to compete with **5**, because the absorption spectra showed a systematic decrease of absorbance from the greatest value in a 1:0 film to the least value in a 1:10 film. The device made of a 1:0 film had, however, a smaller

Table 4. Photovoltaic parameters of **5**-sensitized solar cells with various dye/CDCA ratios under AM 1.5 illumination (power 100 mW cm^{-2}) and active area 0.16 cm^2.

[**5**]:[CDCA]	J_{SC} [mA cm^{-2}]	V_{OC} [mV]	FF	η [%]
1:0	12.22	686	0.645	5.4
1:1	14.33	710	0.594	6.0
1:2	13.22	708	0.640	6.0
1:4	12.05	710	0.662	5.7
1:10	11.23	701	0.668	5.3
N3 dye	12.08	756	0.666	6.1

FULL PAPER

J_{SC} value than those made of the 1:1 and 1:2 films, making the cell performance of the former ($\eta = 5.4\%$) poorer than those of the latter ($\eta = 6.0\%$). Under the highest CDCA concentration (1:10), the small amount of dye loaded onto the TiO$_2$ film resulted in deteriorated cell performance of the device ($\eta = 5.3\%$).

Because our TiO$_2$ films were not optimized to provide an absolute η value for porphyrin **5**, we report a comparison of the cell performance of **5** with the representative dye, **N3**, which is a ruthenium complex-based dye widely used as a reference in DSSC applications ($\eta = 10\%$).[2] Figure 9a shows the spectral maximum of **N3** at 530 nm whereas the Q band of **5** is red-shifted to 650 nm. The I–V curves shown in Figure 9b indicate that the devices made of both 1:1 and 1:2 films have larger J_{SC} values than that made of **N3** film, but the latter has a larger V_{OC} value than the former; both effects balanced to some extent so that the cell performance of the device made of **5** became comparable to that made of **N3** dye. Our compound **5** is thus perhaps the best porphyrin dye reported in the literature, which makes this green dye a promising candidate for colorful DSSC applications.

Conclusion

We have prepared novel porphyrin-based dyes for DSSC applications. Our strategy for the porphyrin design is summarized by three major points: 1) the introduction of *tert*-butyl groups onto phenyl rings tends to suppress the formation of dye aggregates on the TiO$_2$ surface; 2) the extension of π conjugation of the porphyrin ring tends to broaden and to red-shift the Soret and Q bands to improve the light-harvesting effect; and 3) the introduction of an electron-donating group in the *meso* position of the porphyrin ring tends to enhance the charge-separation capability. Among these dyes, a device made of diarylamino-substituted porphyrin **5** adsorbed on a 9 μm TiO$_2$ film exhibits a short-circuit photocurrent density (J_{SC}) of 13.6 mA cm^{-2}, an open-circuit voltage (V_{OC}) of 0.70 V, and a fill factor (*FF*) of 0.63, corresponding to an overall efficiency of power conversion of 6.0%. From our comparison of cell performance with the same TiO$_2$ films, porphyrin **5** outperformed the best reported porphyrin sensitizer and has a performance comparable to that of an **N3**-based DSSC. Work is in progress to modify the structure of the porphyrin-based sensitizer with a more strongly electron-pushing group to increase the efficiency of power conversion, and with hydrophobic long-chain substituents to improve the long-term stability of the device.

Acknowledgements

[1] a) M. K. Nazeeruddin, P. Péchy, M. Grätzel, *Chem. Commun.* **1997**, 1705; b) M. K. Nazeeruddin, S. M. Zakeeruddin, R. Humphry-Baker, M. Jirousek, P. Liska, N. Vlachopoulos, V. Shklover, C.-H. Fischer, M. Grätzel, *Inorg. Chem.* **1999**, *38*, 6298; c) M. K. Nazeeruddin, P. Péchy, T. Renouard, S. M. Zakeeruddin, R. Humphry-Baker, P. Comte, P. Liska, L. Cevey, E. Costa, V. Shklover, L. Spiccia, G. B. Deacon, C. A. Bignozzi, M. Grätzel, *J. Am. Chem. Soc.* **2001**, *123*, 1613.

[2] a) B. O'Regan, M. Grätzel, *Nature* **1991**, *353*, 737; b) M. K. Nazeeruddin, A. Kay, I. Rodicio, R. Humphry-Baker, E. Müller, P. Liska, N. Vlachopoulos, M. Grätzel, *J. Am. Chem. Soc.* **1993**, *115*, 6382.

[3] K. Kalayansundaram, M. Grätzel, *Coord. Chem. Rev.* **1998**, *177*, 347.

[4] a) K. Hara, K. Sayama, Y. Ohga, A. Shinpo, S. Suga, H. Arakawa, *Chem. Commun.* **2001**, 569; b) K. Hara, M. Kurashige, Y. Danoh, C. Kasada, A. Shinpo, S. Suga, K. Sayama, H. Arakawa, *New J. Chem.* **2003**, *27*, 783; c) Z.-S. Wang, Y. Cui, Y. Dan-oh, C. Kasada, A. Shinpo, K. Hara, *J. Phys. Chem. C* **2007**, *111*, 7224.

[5] a) T. Horiuchi, H. Miura, S. Uchida, *Chem. Commun.* **2003**, 3036; b) T. Horiuchi, H. Miura, K. Sumioka, S. Uchida, *J. Am. Chem. Soc.* **2004**, *126*, 12218; c) S. Ito, S. M. Zakeeruddin, R. Humphry-Baker, P. Liska, R. Charvet, P. Comte, M. K. Nazeeruddin, P. Péchy, M. Takata, H. Miura, S. Uchida, M. Grätzel, *Adv. Mater.* **2006**, *18*, 1202.

[6] a) T. Kitamura, M. Ikeda, K. Shigaki, T. Inoue, N. A. Anderson, X. Ai, T. Lian, S. Yanagida, *Chem. Mater.* **2004**, *16*, 1806; b) K. Hara, T. Sato, R. Katoh, A. Furabe, T. Yoshihara, M. Murai, M. Kurashige, S. Ito, A. Shinpo, S. Suga, H. Arakawa, *Adv. Funct. Mater.* **2005**, *15*, 246.

[7] a) S. Kim, H. Choi, D. Kim, K. Song, S. O. Kang, J. Ko, *Tetrahedron* **2007**, *63*, 9206; b) S. Kim, H. Choi, C. Baik, K. Song, S. O. Kang, J. Ko, *Tetrahedron* **2007**, *63*, 11436; c) I. Jung, J. K. Lee, K. H. Song, K. Song, S. O. Kang, J. Ko, *J. Org. Chem.* **2007**, *72*, 3652.

[8] a) M. Velusamy, K. R. J. Thomas, J. T. Lin, Y. Hsu, K. Ho, *Org. Lett.* **2005**, *7*, 1899; b) D. P. Hagberg, T. Edvinsson, T. Marinado, G. Boschloo, A. Hagfeldt, L. Sun, *Chem. Commun.* **2006**, 2245; c) M. Liang, W. Xu, F. Cai, P. Chen, B. Peng, J. Chen, Z. Li, *J. Phys. Chem. C* **2007**, *111*, 4465.

[9] a) S. Ferrere, A. Zaban, B. A. Greg, *J. Phys. Chem. B* **1997**, *101*, 4490; b) S. Ferrere, B. A. Greg, *New J. Chem.* **2002**, *26*, 1155; c) Y. Shibano, T. Umeyama, Y. Matano, H. Imahori, *Org. Lett.* **2007**, *9*, 1971.

[10] a) A. Ehret, L. Stuhl, M. T. Spitler, *J. Phys. Chem. B* **2001**, *105*, 9960; b) S. Ushiroda, N. Ruzycki, Y. Lu, M. T. Spitler, B. A. Parkinson, *J. Am. Chem. Soc.* **2005**, *127*, 5158; c) S. Tatay, S. A. Haque, B. O'Regan, J. R. Durrant, W. J. H. Verhees, J. M. Kroon, A. Vidal-Ferran, P. Gaviña, E. Palomares, *J. Mater. Chem.* **2007**, *17*, 3037.

[11] a) Q.-H. Yao, L. Shan, F.-Y. Li, D.-D. Yin, C.-H. Huang, *New J. Chem.* **2003**, *27*, 1277; b) Y.-S. Chen, C. Li, Z.-H. Zeng, W.-B. Wang, X.-S. Wang, B.-W. Zhang, *J. Mater. Chem.* **2005**, *15*, 1654.

[12] a) K. Hara, T. Sato, R. Katoh, A. Furube, Y. Ohga, A. Shinpo, S. Suga, K. Sayama, H. Sugihaa, H. Arakawa, *J. Phys. Chem. B* **2003**, *107*, 597; b) A. Morandeira, G. Boschloo, A. Hagfeldt, L. Hammarstrolm, *J. Phys. Chem. B* **2005**, *109*, 19403; c) N. Koumura, Z.-S. Wang, S. Mori, M. Miyashita, E. Suzuki, K. Hara, *J. Am. Chem. Soc.* **2006**, *128*, 14256.

[13] *The Photosynthetic Reaction* (Eds.: J. Deisenhofer, J. R. Norris), Academic Press, New York, **1993**.

[14] a) J.-P. Collin, A. Harriman, V. Heitz, F. Odobel, J.-P. Sauvage, *J. Am. Chem. Soc.* **1994**, *116*, 5679; b) J. Seth, V. Palaniappan, R. W. Wagner, T. E. Johnson, J. S. Lindsey, D. F. Bocian, *J. Am. Chem. Soc.* **1996**, *118*, 11194; c) D.-L. Jiang, T. Aida, *J. Am. Chem. Soc.* **1998**, *120*, 10895; d) D. Gust, T. A. Moore, A. L. Moore, *Acc. Chem. Res.* **2001**, *34*, 40; e) H. S. Cho, H. Rhee, J. K. Song, C. K. Min, M. Takase, N. Aratani, S. Cho, A. Osuka, T. Joo, D. Kim, *J. Am. Chem. Soc.* **2003**, *125*, 5849; f) T. V. Duncan, S. P. Wu, M. J. Therien, *J. Am. Chem. Soc.* **2006**, *128*, 10423; g) H. Imahori, *Bull. Chem. Soc. Jpn.* **2007**, *80*, 621; h) M. U. Winters, J. Kärnbratt, H. E. Blades, C. J. Wilson, M. J. Frampton, H. L. Anderson, B. Albinsson, *Chem. Eur. J.* **2007**, *13*, 7385.

[15] a) J. N. Clifford, G. Yahioglu, L. R. Milgrom, J. R. Durrant, *Chem. Commun.* **2002**, 1260; b) T. Hasobe, H. Imahori, P. V. Kamat, T. K. Ahn, S. K. Kim, D. Kim, A. Fujimoto, T. Hirakawa, S. Fukuzumi, *J.*

Am. Chem. Soc. **2005**, *127*, 1216; c) T. Hasobe, P. V. Kamat, V. Troiani, N. Solladié, T. K. Ahn, S. K. Kim, D. Kim, A. Kongkanand, S. Kuwabata, S. Fukuzumi, *J. Phys. Chem. B* **2005**, *109*, 19; d) M. Borgström, E. Blart, G. Boschloo, E. Mukhtar, A. Hagfeldt, L. Hammarström, F. Odobel, *J. Phys. Chem. B* **2005**, *109*, 22928; e) L. Luo, C.-F. Lo, C.-Y. Lin, I-J. Chang, E. W.-G. Diau, *J. Phys. Chem. B* **2006**, *110*, 410; f) A. Huijser, T. J. Savenije, A. Kotlewski, S. J. Picken, L. D. A. Siebbeles, *Adv. Mater.* **2006**, *18*, 2234; g) O. Hagemann, M. Jørgensen, F. C. Krebs, *J. Org. Chem.* **2006**, *71*, 5546; h) G. M. Hasselman, D. F. Watson, J. R. Stromberg, D. F. Bocian, D. Holten, J. S. Lindsey, G. J. Meyer, *J. Phys. Chem. B* **2006**, *110*, 25430; i) S. Eu, S. Hayashi, T. Umeyama, A. Oguro, M. Kawasaki, N. Kadota, Y. Matano, H. Imahori, *J. Phys. Chem. C* **2007**, *111*, 3528.

[16] a) B. C. O'Regan, I. Lo'pez-Duarte, M. V. Martý'nez-Dý'az, A. Forneli, J. Albero, A. Morandeira, E. Palomares, T. Torres, J. R. Durrant, *J. Am. Chem. Soc.* **2008**, *130*, 2906; b) J.-J. Cid, J.-H. Yum, S.-R. Jang, M. K. Nazeeruddin, E. Martínez-Ferrero, E. Palomares, J. Ko, Michael Grätzel, T. Torres, *Angew. Chem.* **2007**, *119*, 8510; *Angew. Chem. Int. Ed.* **2007**, *46*, 8358; c) P. Y. Reddy, L. Giribabu, C. Lyness, H. J. Snaith, C. Vijaykumar, M. Chandrasekharam, M. Lakshmikantam, J.-H. Yum, K. Kalyanasundaram, M. Grätzel, M. K. Nazeer, *Angew. Chem.* **2007**, *119*, 441; *Angew. Chem. Int. Ed.* **2007**, *46*, 437; d) J. He, G. Benkö, F. Korodi, T. Polívka, R. Lomoth, B. Åkermark, L. Sun, A. Hagfeldt, V. Sundström, *J. Am. Chem. Soc.* **2002**, *124*, 4922; e) E. Palomares, M. V. Martínez-Díaz, Saif A. Haque, T. Torres, J. R. Durrant, *Chem. Commun.* **2004**, 2112.

[17] a) W. M. Campbell, A. K. Burrell, D. L. Officer, K. W. Jolley, *Coord. Chem. Rev.* **2004**, *248*, 1363; b) Q. Wang, W. M. Campbell, E. E. Bonfantani, K. W. Jolley, D. L. Officer, P. J. Walsh, K. Gordon, R. Humphry-Baker, M. K. Nazeeruddin, M. Grätzel, *J. Phys. Chem. B* **2005**, *109*, 15397; c) L. Schmidt-Mende, W. M. Campbell, Q. Wang, K. W. Jolley, D. L. Officer, M. K. Nazeeruddin, M. Grätzel, *ChemPhysChem* **2005**, *6*, 1253; d) W. M. Campbell, K. W. Jolley, P. Wagner, K. Wagner, P. J. Walsh, K. C. Gordon, L. Schmidt-Mende, M. K. Nazeeruddin, Q. Wang, M. Grätzel, D. L. Officer, *J. Phys. Chem. C* **2007**, *111*, 11760.

[18] a) T. Hasobe, S. Fukuzumi, S. Hattori, P. V. Kamat, *Chem. Asian J.* **2007**, *2*, 265; b) S. Eu, S. Hayashi, T. Umeyama, A. Oguro, M. Kawasaki, N. Kadota, Y. Matano, H. Imahori, *J. Phys. Chem. C* **2007**, *111*, 3528; c) J. Rochford, D. Chu, A. Hagfeldt, E. Galoppini, *J. Am. Chem. Soc.* **2007**, *129*, 4655.

[19] C. Luo, D. M. Guldi, H. Imahori, K. Tamaki, Y. Sakata, *J. Am. Chem. Soc.* **2000**, *122*, 6535.

[20] a) D. Liu, R. W. Fessenden, G. L. Hug, P. V. Kamat, *J. Phys. Chem. B* **1997**, *101*, 2583; b) S. Kim, J. K. Lee, S. O. Kang, J. Ko, J.-H. Yum, S. Fantacci, F. D. Angelis, D. D. Censo, M. K. Nazeeruddin, M. Grätzel, *J. Am. Chem. Soc.* **2006**, *128*, 16701.

[21] a) V. S.-Y. Lin, S. G. Di Magno, M. J. Therien, *Science* **1994**, *264*, 1105; b) V. S.-Y. Lin, M. J. Therien, *Chem. Eur. J.* **1995**, *1*, 645; c) P. N. Taylor, J. Huuskonen, G. Rumbles, R. T. Aplin, E. Williams, H. L. Anderson, *Chem. Commun.* **1998**, 909; d) K. Nakamura, T. Fujimoto, S. Takara, K.-I. Sugiura, H. Miyasaka, T. Ishii, M. Yamashita, Y. Sakata, *Chem. Lett.* **2003**, *32*, 694; e) H. L. Anderson, S. J. Martin, D. D. C. Bradley, *Angew. Chem.* **1994**, *106*, 711; *Angew. Chem. Int. Ed. Engl.* **1994**, *33*, 655; f) A. Osuka, N. Tanabe, S. Kawabata, I. Yamazaki, Y. Nishimura, *J. Org. Chem.* **1996**, *61*, 7177; g) K. Maruyama, S. Kawabata, *Bull. Chem. Soc. Jpn.* **1990**, *63*, 170; h) P. N. Taylor, H. L. Anderson, *J. Am. Chem. Soc.* **1999**, *121*, 11538.

[22] a) R. W. Wagner, T. E. John, F. Li, J. S. Lindsey, *J. Org. Chem.* **1995**, *60*, 5266; b) T. E. O. Screen, K. B. Lawton, G. S. Wilson, N. Dolney, R. Ispasoiu, T. Goodson III, S. J. Martin, D. D. C. Bradley, H. L. Anderson, *J. Mater. Chem.* **2001**, *11*, 312; c) M.-C. Kuo, L.-A. Li, W.-N. Yen, S.-S. Lo, C.-W. Lee, C.-Y. Yeh, *Dalton Trans.* **2007**, 1433.

[23] a) K. Hara, K. Sayama, Y. Ohga, A. Shinpo, S. Suga, H. Arakawa, *Chem. Commun.* **2001**, 569; b) K. Hara, M. Kurashige, S. Ito, A. Shinpo, S. Suga, K. Sayama, H. Arakawa, *Chem. Commun.* **2003**, 252.

[24] T.-G. Zhang, Y. Zhao, I. Asselberghs, A. Persoons, K. Clays, M. J. Therien, *J. Am. Chem. Soc.* **2005**, *127*, 9710.

[25] Y. Chen, X. P. Zhang, *J. Org. Chem.* **2003**, *68*, 4432.

[26] S.-L. Li, K.-J. Jiang, K.-F. Shao, L.-M. Yang, *Chem. Commun.* **2006**, 2792.

[27] J. P. C. Tomé, A. M. V. M. Pereira, C. M. A. Alonso, M. G. P. M. S. Neves, A. C. Tomé, A. M. S. Silva, J. A. S. Cavaleiro, M. V. Martínez-Díaz, T. Torres, G. M. Aminur Rahman, J. Ramey, D. M. Guldi, *Eur. J. Org. Chem.* **2006**, *2006*, 257.

[28] a) X. Zhou, K. S. Chan, *J. Org. Chem.* **1998**, *63*, 99; b) K. S. Chan, X. Zhou, M. T. Au, C. Y. Tam, *Tetrahedron* **1995**, *51*, 3129.

[29] a) J.-C. Chang, C.-J. Ma, G.-H. Lee, S.-M. Peng, C.-Y. Yeh, *Dalton Trans.* **2005**, 1504; b) W.-N. Yen, S.-S. Lo, M.-C. Kuo, C.-L. Mai, G.-H. Lee, S.-M. Peng, C.-Y. Yeh, *Org. Lett.* **2006**, *8*, 4239.

[30] D. F. Rohrbach, E. Deutsch, W. R. Heineman, R. F. Pasternack, *Inorg. Chem.* **1977**, *16*, 2650.

[31] P. Wang, S. M. Zakeeruddin, P. Comte, R. Charvet, R. Humphry-Baker, M. Grätzel, *J. Phys. Chem. B* **2003**, *107*, 14336.

[32] S. Ito, P. Chen, M. K. Nazeeruddin, P. Liska, P. Péchy, M. Grätzel, *Prog. Photovolt.: Res. Appl.* **2007**, *15*, 603.

[33] S. Ito, H. Matsui, K. Okada, S. Kusano, T. Kitamura, Y. Wada, S. Yanagida, *Sol. Energy Mater. Sol. Cells* **2004**, *82*, 421.